Journal of Corrosion and Materials *J. Corros. Mater.* (2022) 1(1), 42–57.
www.corromat.com

Robust Lyapunov Certification of Fading-Memory Corrosion Dynamics with Generalized Proportional Caputo Derivatives

Steven M. Zelditch[1,*], Michael Reynolds[2]

[1] *Department of Mathematics, Northwestern University, Evanston, IL 60208, USA*
[2] *Department of Mechanical Engineering, Massachusetts Institute of Technology, Cambridge, MA 02139-4307, USA*

[*] Corresponding author: zelditch@math.northwestern.edu
[2] reynoldsmichael260@gmail.com

(Received: 13 February 2022. Received in revised form: 28 April 2022. Accepted: 15 May 2022. Published online: 30 June 2022.)

Abstract

Corrosion-degradation models may be applied to systems where current degradation state depends on past exposures and cyclic environment forcing. Fractional derivative models are fit to such cases as they maintain memory. However, a memory-filled model alone cannot be considered as a reliability certificate. The analysis of a service-oriented model also requires specification of whether any bounded uncertainty in electrolyte chemistry, temperature, wetness history, oxygen access or measurement noise is also bounded in the chosen damage variables. The core of the problem is to verify whether the generalized proportional Caputo system can give a Lyapunov certificate that would link fading memory, bounded environmental disturbances and corrosion-state boundedness. In this analysis, the comparison theorem for non-autonomous nonlinear fractional order systems with generalized Caputo derivatives is formulated and used to analyze a two-state example of a numerical corrosion process. The model is constructed based on the stated equations with $\alpha \in \{0.55, 0.70, 0.85\}$, $\rho \in \{0.70, 0.85, 0.90, 0.95, 1.00\}$, $x(0) = (0.52, 0.52)^\top$, $g(t) = -1 + 0.25\sin(0.3t)$, $\delta \in \{0, 0.01, 0.03, 0.05\}$, $T = 40$ and $h = 0.02$. The results imply that the proportional parameter ρ serves as a stability-related memory parameter and not just as a tuning one. With $\delta = 0.03$, for example, the case of $(\alpha, \rho) = (0.70, 0.70)$ attains the threshold of $\|x\| < 0.05$ at approximately $t = 13.6$, while the case with the same α and $\rho = 0.95$ does not attain the threshold even at $T = 40$. As ρ varies from 0.70 to 0.95 with the same disturbance amplitude, robust certificate radii grow from 0.200 to 1.200. Another nonlinear saturation kinetics evaluation gives a radius of about 0.084 for $r = 0.75$, $a = 0.40$, and $\delta = 0.03$. It is found from the investigation that generalized proportional Caputo derivatives have applications in evaluating corrosion behavior only when memory parameter, disturbance supply, and Lyapunov constants are mentioned together.

Keywords: corrosion degradation; generalized proportional Caputo derivative; fractional stability; Lyapunov certificate; practical boundedness; disturbed materials models.

1. Introduction

Corrosion process is path dependent. A surface under conditions of exposure to chloride ions, moisture, oxygen and varying temperatures reacts not just to the final state of the electrolyte. Previous wetting periods, rupture of a passive film, acidification of the environment, precipitation of corrosion products, limitations in transport, biological processes, inhibition and mechanical removing of a deposit can affect the rate and location of corrosion at the moment of observation. The pitting theory based on a transport approach combines local chemistry, reaction rate and film properties with concentrated corrosion damage [1]. Critical review of pitting corrosion further clarifies the importance of small local changes in a system [2]. General corrosion theory describes the effect of electrolyte access, electrochemical kinetics and surface properties [3]. Surface chemistry methods explain the correlation between corrosion reaction rate and the state of interface [4]. Corrosion science provides a link between a corrosion rate and other variables like local chemistry and surface evolution [5]. Theory of atmospheric corrosion describes the role of moisture, pollution and product layer transport in a long-term process [6]. A curve obtained from fitting mass loss or current density may describe a particular period of observation, however, it will not answer the reliability question of corrosion engineering: whether small deviations from a state and bounded variations of the forcing stay bounded.

The difference between the curve fitting and boundedness is crucial for a corrosion reliability analysis. While the deterministic degradation law is important for service life estimation, it does not describe the sensitivity to the bounded disturbances in an environment. In a corrosion system, bounded disturbances can occur due to chloride pulses, pH variation, wet–dry cycles, temperature fluctuation, oxygen access, variability in preparation of the surface and sensor noise. Therefore, the engineering task is not only a presence of a stable unforced equilibrium, but also existence of a finite ultimate radius in the selected damage variables caused by a persistent admissible forcing. Practical stability is preferable over ideal asymptotic stability since the real histories of the environmental exposures are not quiescent. Modelling of marine immersion corrosion showed that the corrosion process may develop in a stage-dependent manner rather than in a single-rate regime [7]. The early seawater corrosion research also described the dependence of the initial rate on oxygen access and surface evolution [8]. The anaerobic bacteria activity also can change the histories of mild steel corrosion in a marine environment [9]. Corrosion engineering also considers the field exposure as a coupled environment and material problem, not as a memoryless rate process [10].

The localized corrosion process makes the stability question more acute than it would be for a homogeneous material loss. A low rate may become dangerous if it leads to pitting or localized corrosion, while the higher rate which is distributed over the surface may be less significant for a specific structural element. The classical theory of pitting provides a link between local chemistry, hydrolysis, transport and passivity breakdown and concentrated defect growth [1]. The modern theory of pitting corrosion stresses the importance of local conditions even if the average reaction rate is low [2]. The discussion of pitting corrosion process also emphasizes that spatial localization should be taken into account separately from the material loss [11]. The corrosion control manuals consider distribution of damage as an important factor of service assessment [12]. An example of corrosion of reinforced concrete also shows this point. The threshold level of chloride ions reviews show that the depassivation depends on exposure, pore chemistry and moisture [13]. The corrosion of concrete literature also discusses the chloride ingress, steel depassivation and cracking in long-term exposure histories [14]. Thus, a damage variable which ignores the memory effect cannot describe the true damage state.

The certificate-based approach does not eliminate the necessity of electrochemical experiments, but it provides another kind of statement. The polarization curves, impedance spectra, pit depth measurement and microscopic observation are descriptions of what was observed. A Lyapunov certificate asks how a given state equation will behave under admissible perturbations. In a peer-reviewed corrosion modelling, it is an important issue since the fractional derivative can provide a realistic curve without the response to bounded perturbations. In the following analysis, the boundedness, clearance time and practical radius are the main outputs rather than some technical details of the mathematical theory.

Fractional differential equations provide an elegant way to incorporate the memory into the system which has a distribution of reaction times or anomalous transport. The Caputo's model provides a description of the nearly frequency independent dissipation via fractional calculus [15]. The classical theory of fractional calculus is the source of the operators used in fractional differential equations [16]. The fractional integrals and derivatives were systematically analyzed and applied to problems [17]. The fractional differential equations provide a general theory of initial value problem with memory [18]. The theory of fractional operators and their applications was further developed [19]. The modern theoretical approaches clarify the importance of proper handling of solution regularity and memory kernels [20]. The fractional models are widely used in physical applications with memory and anomalous relaxation [21]. The fractional kinetic equations are used in anomalous diffusion when the transport is not Brownian [22]. The continuous-time random walk model is another way of derivation of the fractional equation from the trapping mechanism [23]. The electrochemical impedance theory relates the constant phase angle to the distributed interfacial response [24]. The linear viscoelasticity theory is another example of memory in the materials response [25]. These aspects make the fractional model suitable for description of corrosion when the surface film, corrosion product or electrolyte path has memory.

The physical meaning of the Mittag–Leffler function is also important for understanding its usage. The exponential relaxation has one characteristic time, whereas Mittag–Leffler relaxation can describe slower decay and a wide range of time scales. The viscoelastic fractional models illustrate how such relaxation represents broad effects of memory [25]. The theory of Mittag–Leffler functions clarifies the analytical background of this relaxation [26]. The complete monotonicity results clarify the cases when the Mittag–Leffler relaxation has a physical interpretation [27]. In the case of corrosion, the distribution of time scales can be caused by the population of surface sites, tortuosity of the corrosion product layer, heterogeneous access of the electrolyte or the mixed control by activation and diffusion. Thus, the use of fractional derivative should be motivated by a physical reason of memory formation rather than an improvement of the numerical fit.

The problem of using the classical fractional models for the corrosion process still exists. The ordinary Caputo kernel has an algebraic memory tail, while many surfaces have fading memory. The chloride pulse may be partly forgotten after repassivation; the inhibitor may be adsorbed and the importance of previous exposure can be changed; the porous corrosion product layer can keep the aggressive ions, but with attenuation; the mechanical cleaning can partly reset the surface history. The generalized proportional derivatives provide a possibility to combine the local proportional behaviour and fractional memory [28]. The corresponding Gronwall inequality allows to obtain an estimate for a perturbed system with the help of the generalized proportional memory [29]. The Laplace transform representation further clarifies the operator in the generalized proportional fractional equation [30]. Thus, the generalized proportional Caputo derivative is a way to satisfy the requirement to model the fading memory by adding the exponential tempering parameter ρ to the kernel of the operator. If $\rho = 1$, the Caputo form is recovered; if $0 < \rho < 1$, the older exposure becomes exponentially less important.

This is not only a numerical adjustment. It changes the memory window and thus, the stability envelope over a finite time interval of inspection.

The Lyapunov analysis provides the certification layer which the fractional model lacks. The stability results for fractional differential equations provide an early foundation for this analysis [31]. The Mittag–Leffler stability is a generalization of the classical exponential stability for fractional-order systems [32]. The Lyapunov direct method provides the approach to the nonlinear fractional dynamics [33]. The fractional transfer functions analysis helps to understand the effect of non-integer order on system stability [34]. The additional stability results help to establish the connection between the fractional model and Lyapunov comparison arguments [35]. The Lyapunov theory for fractional differential equations was developed using the comparison and the direct methods [36]. The control-oriented results extend these ideas to the fractional nonlinear systems [37]. The practical stability theory studies the connection between bounded forcing and the response of the fractional system [38]. The fractional-order stability analysis reveals the importance of admissible perturbations [39]. The delay and fractional effects can be combined using the proper Lyapunov structures [40]. The existence and stability results provide the mathematical ground for the new kernel class of generalized proportional operators [41]. The generalized proportional equations were also studied using the transform and solution estimates [42]. The stability of these equations can be analyzed using the Gronwall-type estimates and the comparison arguments [43]. The further analysis of proportional fractional operators reveals the relation with the classical fractional calculus [44]. The quadratic Lyapunov functions provide the certificate form for generalized proportional dynamics [45]. These mathematical tools are used to formulate the corrosion-degradation problem: is it possible to describe the fading memory and bounded forcing in terms of certificate constants?

The research question is formulated deliberately narrowly. It asks whether the generalized proportional Caputo model of corrosion degradation can provide the Lyapunov certificate which connects the fading memory, bounded environmental disturbance and boundedness of the state variables. Such a model should not only provide a good fit of the degradation curve. It should include the explicit disturbance-to-state relationship, which can be verified from the certificate. Therefore, the analysis treats the memory parameter, disturbance amplitude and Lyapunov supply rate as declared variables.

The conceptual pathway of Figure 1 reflects this interpretation. The environmental inputs and exposure history provide the forcing of a fractional equation, the generalized proportional kernel defines the fading memory and the Lyapunov inequality transforms the state equation to the degradation bound.

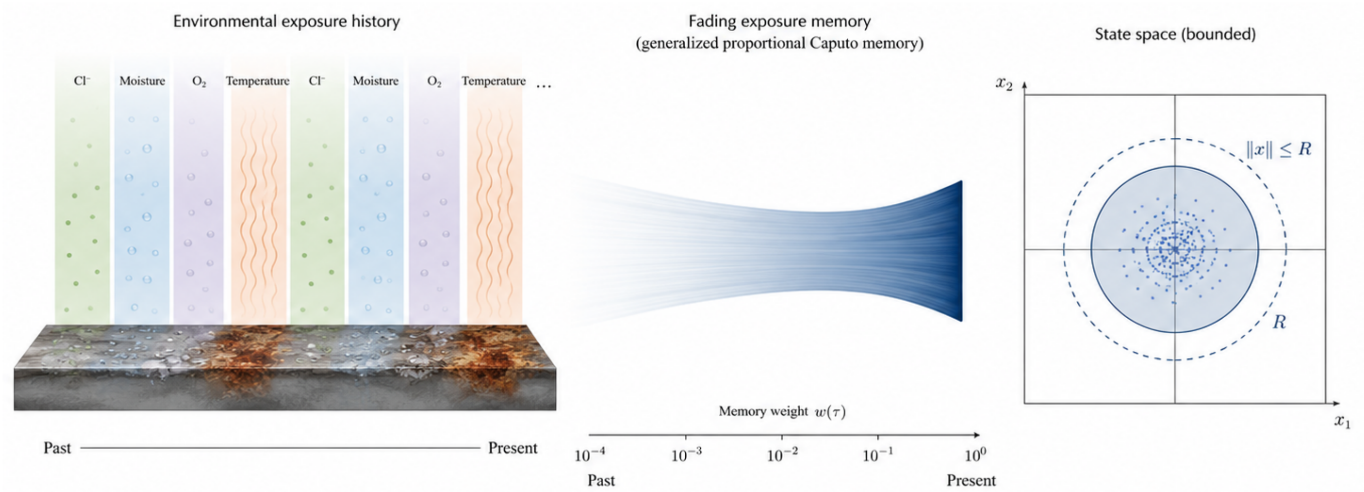

Figure 1: Fading exposure memory.

Moreover, the map shown in Fig. 1 explains why the experiment involves a numerical simulation rather than an empirical calibration cycle. In this case, the goal is not to estimate the corrosion parameters for a given alloy, coating, or electrolyte. The goal is to examine the transition from the specified fractional equation to the specified robust bound. In order to perform such a test, it is necessary to ensure that the equations remain clear enough to recalculate every figure, table, and certificate radius.

The idea of the certificate is also reflected in the way how the state vector is defined. For instance, when the state variable is a pit depth measurement, an impedance-based film parameter, or a normalized local penetration index, it is necessary to guarantee that the zero state corresponds to a reference configuration. If the state variable is some kind of transformation, the ordering property is preserved in order to make a valid statement about the safety. The requirement is standard in nonlinear stability analysis, but it is often neglected in empirical degradation modeling. Therefore, the normalized variables are used explicitly to characterize the surface film imbalance and local depth perturbation.

2. Generalized proportional Caputo model

Let $0 < \alpha < 1$, $\rho \in (0, 1]$ and $t > t_0$. The generalized proportional fractional integral used in the analysis is

$$({}_{t_0}I^{\alpha,\rho}u)(t) = \frac{1}{\rho^\alpha \Gamma(\alpha)} \int_{t_0}^{t} \exp\left(\frac{\rho - 1}{\rho}(t - s)\right)(t - s)^{\alpha-1} u(s)\,\mathrm{d}s. \tag{1}$$

The associated Caputo-type generalized proportional derivative is

$$({}^{C}_{t_0}D^{\alpha,\rho}u)(t) = ({}_{t_0}I^{1-\alpha,\rho}D^{1,\rho}u)(t), \qquad D^{1,\rho}u(t) = (1 - \rho)u(t) + \rho\dot{u}(t). \tag{2}$$

The kernel defined in Eq. (1) has the algebraic term $(t-s)^{\alpha-1}$ and the exponential factor $\exp((\rho-1)(t-s)/\rho)$. The order α determines the strength of the near-present singular memory contribution, whereas ρ controls the decay of older exposure. For $\rho = 1$, there is no exponential factor, and the operator collapses back into the standard Caputo memory kernel. With $0 < \rho < 1$, the old part of the exposure memory is tempered.

The memory window depicted in Figure 2 indicates the effect of the proportional parameter on the normalized kernel for $\alpha = 0.70$. Lower ρ values result in the decay of remote history having a stronger effect. In terms of corrosion, this represents a case where passivation, surface renewal, or reaction product rearrangement or electrolyte replacement has diminished the effects of older exposure to an aggressive environment. Higher ρ values represent an increased memory and hence a more durable surface.

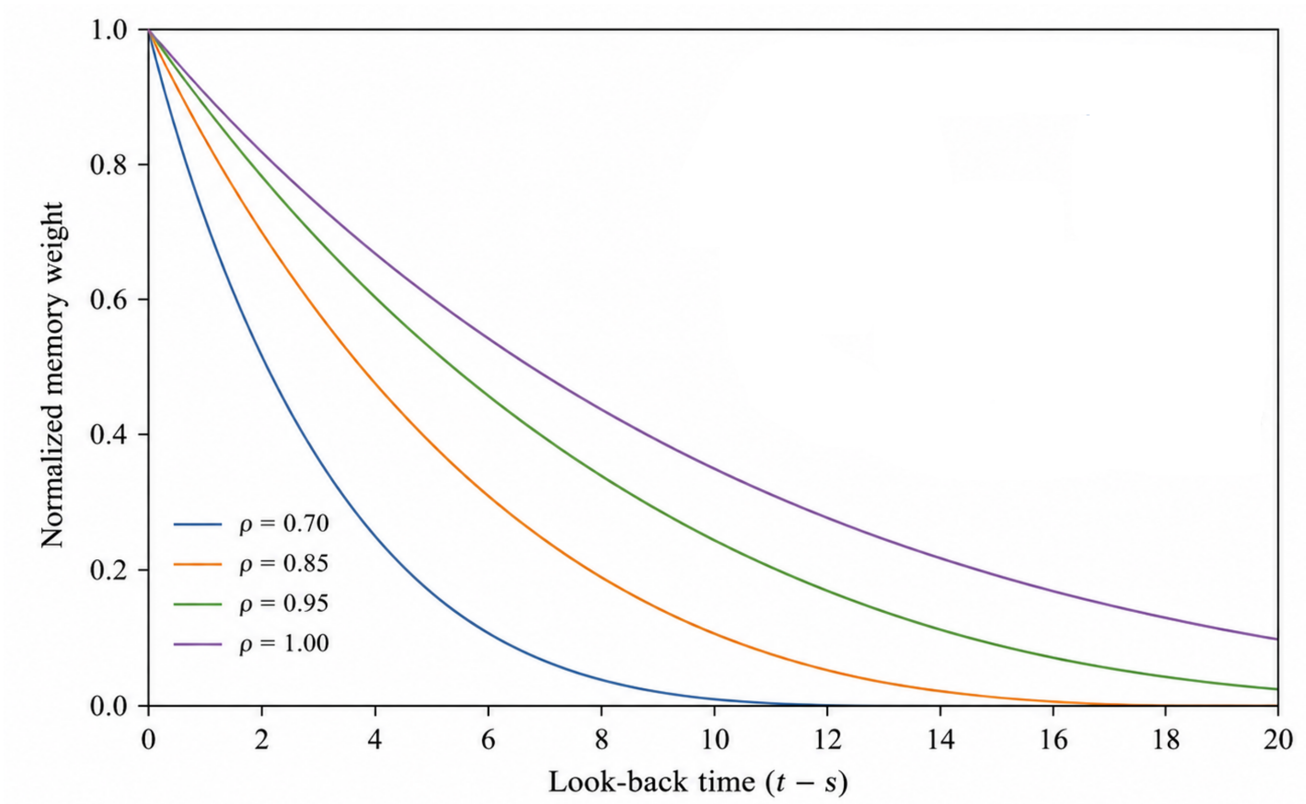

Figure 2: Tempered memory kernel.

The kernel plot in Fig. 2 makes the disclosure implication inescapable. For two models having the same α value but differing ρ values, the history of exposures is not the same. If the order α was specified alone, as might happen in some corrosion experiments, then the memory horizon would remain unspecified. The parameter ρ determines if any past chloride, wet–dry or temperature change event survives into the later state of degradation. It is thus both a mathematical parameter and a modelling assumption about physical behavior.

With two memory parameters there is an especially convenient way to distinguish two phenomena that are sometimes confused. The parameter α modifies the fractional relaxation law while ρ modifies the past by exponentially tempering it. When considering the finite-horizon aspect of corrosion modeling, those two phenomena are not equivalent. By lowering α, one can reduce fractional relaxation, but lower ρ means even more aggressive removal of past events. Hence the model allows for a deeper interpretation than the single-order fractional equation; this requires proper justification of both parameters.

The degradation process of interest here takes the general form

$${}^{C}_{t_0}D^{\alpha,\rho}x(t) = f(t, x(t)) + G(t)d(t), \qquad x(t_0) = x_0, \tag{3}$$

where $x(t) \in \mathbb{R}^n$ is a vector of normalized degradation variables, $d(t)$ is a bounded environmental or measurement disturbance and $G(t)$ is a bounded input map. The coordinates in the state vector may stand for perturbations of corrosion potential, oxide film imbalance, normalized pit depth difference from the average value, soluble product concentration or some abstract degradation coordinates relative to the nominal state. There is no need for each coordinate to have a definite physical interpretation but the zero vector should represent an accepted reference state.

The certificate will be required to satisfy bounds in terms of a comparison pair

$$a_1(\|x\|) \leq V(t, x) \leq a_2(\|x\|), \qquad (t, x) \in [t_0, \infty) \times \Delta, \tag{4}$$

for some class-$\mathcal{K}$ functions a_1 and a_2. These bounds supply a materials interpretation for the certificate: V needs to increase with respect to the magnitude of the degradation-state vector. A scalar which can take on a small value even when the state variable takes on a large value cannot represent a measure of damage. The bounds also make it possible to convert a Lyapunov bound into a state bound.

Moreover, the use of comparison functions in Eq. (4) has something to do with the stability convention beyond mere formality. It ensures that there will be no mismatch between the certificate and the degradation state. In case the chosen Lyapunov function is dominated by one coordinate but ignores another, it may happen that a small certificate will correspond to a large physical damage state. For the purposes of the next section, the choice of a quadratic certificate $V = x_1^2 + x_2^2$ prevents such mismatch because both normalized coordinates enter the certificate directly.

For the scalar comparison equation

$${}_{t_0}^{C}D^{\alpha,\rho} y(t) = -cy(t), \qquad y(t_0) = y_0, \tag{5}$$

the homogeneous decay envelope is

$$y(t) = y_0 \Phi_{\alpha,\rho,c}(t - t_0), \qquad \Phi_{\alpha,\rho,c}(\tau) = \exp\left(\frac{\rho - 1}{\rho}\tau\right) E_\alpha\left[-c\left(\frac{\tau}{\rho}\right)^\alpha\right]. \tag{6}$$

The exponential part in Eq. (6) captures the behavior of finite-horizon fading memory. The Mittag-Leffler part represents fractional relaxation; ρ controls both memory decay and relaxation argument. Numerical integration of fractional memory functions can be done via convolution quadrature, e.g., [46]; another common choice is predictor-corrector schemes [47]. Special functions can be computed using Mittag-Leffler algorithms [48]. Computations are performed by evaluating the envelope as a certificate object rather than curve fitting.

3. Lyapunov certificate under environmental forcing

The inequality ${}_{t_0}^{C}D^{\alpha,\rho} V \leq -cV$ without the right-hand side is insufficient for corrosion problems since environmental fluctuations never disappear. The certificate we use allows nonnegative supply,

$${}_{t_0}^{C}D^{\alpha,\rho} V(t, x(t)) \leq -cV(t, x(t)) + q(t), \qquad c > 0, \tag{7}$$

where $q(t)$ is the bound on the Lyapunov-level disturbance. This is not a new source of corrosion; rather, it is the consequence of bounding the input and using the state to estimate the product with an inequality of the Young type. The value of Eq. (7) is that it reveals how much nominal decay is sacrificed for the sake of robustness.

For the case where the supply is tempered according to $q(t) \leq \bar{q} \exp((\rho - 1)(t - t_0)/\rho)$, comparison yields

$$V(t, x(t)) \leq V(t_0, x_0)\Phi_{\alpha,\rho,c}(t - t_0) + \bar{q}\Psi_{\alpha,\rho,c}(t - t_0), \tag{8}$$

because the positivity of the generalized proportional kernel implies that the first term in Eq. (8) is the homogeneous certificate, while the second term is the accumulated influence of the disturbance. The function in Eq. (8) is bounded since the kernel is nonnegative and the state-dependent bounds in Eq. (4) allow the scalar estimate to be converted to a state estimate.

The case of the tempered supply has an interpretation in terms of corrosion. It is a disturbance filtered with the same fading exposure process as the state equation. A chloride spike followed by repassivation, measurement noise filtered through a surface memory model, or an environment perturbation decayed by electrolyte layer renewal can yield this form. The certificate shows that forcing with such disturbances does not change the response envelope but does not ruin finite horizon boundedness.

The untempered persistent forcing case is more difficult since if $q(t) \leq \bar{q}$ is untempered, the memory weighted gain must be carried explicitly:

$$V(t, x(t)) \leq V(t_0, x_0)\Phi_{\alpha,\rho,c}(t - t_0) + \bar{q}G_{\alpha,\rho,c}(t - t_0), \tag{9}$$

with

$$G_{\alpha,\rho,c}(\tau) = \frac{1}{\rho^\alpha}\int_0^\tau \exp\left(\frac{\rho-1}{\rho}(\tau-s)\right)(\tau-s)^{\alpha-1}E_{\alpha,\alpha}\left[-c\left(\frac{\tau-s}{\rho}\right)^\alpha\right]\mathrm{d}s. \tag{10}$$

The gain translates an everlasting disturbance to a practical degradation neighbourhood. In the context of field exposure, the latter is the proper object because the chloride concentration, the wetness, the temperature and the oxygen are never equal to zero. Hence, we obtain the disturbance-to-state bound in the following form:

$$\limsup_{t\to\infty}\|x(t)\| \le R(\|d\|_\infty). \tag{11}$$

The framework of input-to-state stability provided a way of describing the effect of bounded inputs for nonlinear systems in control-theoretic terms [49]. Lyapunov characterizations of input-to-state stability relate input and state bounds [50]. Then the theory of nonlinear systems provides a language of practical stability to describe ultimate boundedness [51]. This construction is close to input-to-state stability concepts from the theory of nonlinear control, but it is based on the memory with fractional order and the proportional kernel.

The interpretation of Eq. (11) as the corrosion tolerance bound normalized by a factor is very convenient. The model does not postulate vanishing disturbance but claims that its effect can be translated to the radius of the bound. Such an approach better fits practice, where some inspection threshold or maximum allowable defect size is assumed for material. The mathematical radius is not directly related to an engineering allowable one, but this correspondence can be established if laboratory and field data provide the scaling of state space.

If the certificates are quadratic, the supply rate becomes inspectable. Let us consider $V = x^\top P x$, where $P = P^\top > 0$, and the nominal dynamics satisfy

$$2x^\top P f(t,x) \le -\lambda V \tag{12}$$

for some $\lambda > 0$. If $\left\|P^{1/2}G(t)\right\| \le \bar{g}$, then for any $\eta \in (0,\lambda)$,

$${}_{t_0}^{C}D^{\alpha,\rho}V \le -(\lambda-\eta)V + \frac{\bar{g}^2}{\eta}\|d(t)\|^2. \tag{13}$$

The certificate involves $2x^\top PGd \le \eta x^\top Px + \eta^{-1}\left\|P^{1/2}Gd\right\|^2$. In this relation, the parameter η is a means of dividing up the gain into supply multiplier η^{-1} and nominal decay rate η. A larger η will lead to a smaller supply multiplier and reduced decay rate; a smaller η will do the opposite.

That trade-off should be noted because different values of η might generate different practical radii from one and the same state equation.

The present certificate is inherently conservative. It assumes maximum possible correlation between the disturbance and the Lyapunov gradient, whereas the real-life disturbances might not always force the state to change in the most harmful manner. In applications, this conservatism is not necessarily an undesirable trait, provided that it is open and documented. When the corrosion model explicitly states the values of c, $\bar{q}$, η, α and ρ, the readers have the possibility of evaluating how much of an overestimate it is. A model which supplies just a fitted trajectory lacks this possibility.

4. Governing degradation equations and certificate constants

The numerical example is based on explicit degradation equations. It is not a laboratory experiment and does not give estimates of kinetic constants for any particular alloy, coating and electrolyte. This is crucial for the following reason: the objective of the exercise is to see if the Lyapunov certificate works consistently under variation of the governing parameters within the grid range. All numerical values are obtained using the stated governing equations, initial condition, disturbance amplitude and fractional parameters.

The governing-equation design also eliminates an ambiguity that is sometimes encountered when dealing with synthetic corrosion. If the numerical example is not provided along with the governing equation, the reader has no opportunity to determine whether the peculiarities of behavior are due to the fractional operator or to some unspoken damping mechanism. Here all coupling, dissipation and forcing are clearly exposed; therefore, the numerical example is suitable for the analysis of the certificate's consistency in the general case.

The two-state model is

$${}_{t_0}^{C}D^{\alpha,\rho}x_1(t) = -\kappa_\rho(t)x_1(t) - g(t)x_2(t) + d_1(t), \tag{14}$$

$${}_{t_0}^{C}D^{\alpha,\rho}x_2(t) = g(t)x_1(t) - \kappa_\rho(t)x_2(t) + d_2(t), \tag{15}$$

where

$$\kappa_\rho(t) = (1-\rho)\frac{1+t^2}{t^2+2}, \qquad g(t) = -1 + 0.25\sin(0.3t). \tag{16}$$

These are taken to be a normalized imbalance in the surface film and a normalized depth perturbation. The skew-symmetric component $g(t)$ exchanges energy between the coordinates but does not add to the quadratic damage index, whereas the dissipative part $\kappa_\rho(t)$ is given by $\kappa_\rho(t)$. The perturbation for calculating the tempered-forced response is

$$d(t) = \delta \exp\left(\frac{\rho - 1}{\rho}(t - 0)\right) \begin{bmatrix} \sin(0.8t) \\ \cos(0.6t) \end{bmatrix}. \tag{17}$$

The trigonoquantity accounts for environmental cycling, and the exponential term ensures the forcing is properly matched to the fading memory of the operator. The coefficient δ is the stated disturbance strength.

The dynamics are illustrated in Figure 3. The cross-coupling cannot be considered as an uncontrollable growth process when using the damage potential $V = x_1^2 + x_2^2$. It is a reversible exchange term that cancels in the quadratic balance. The dissipative diagonal contribution and the disturbance supply determine the certificate.

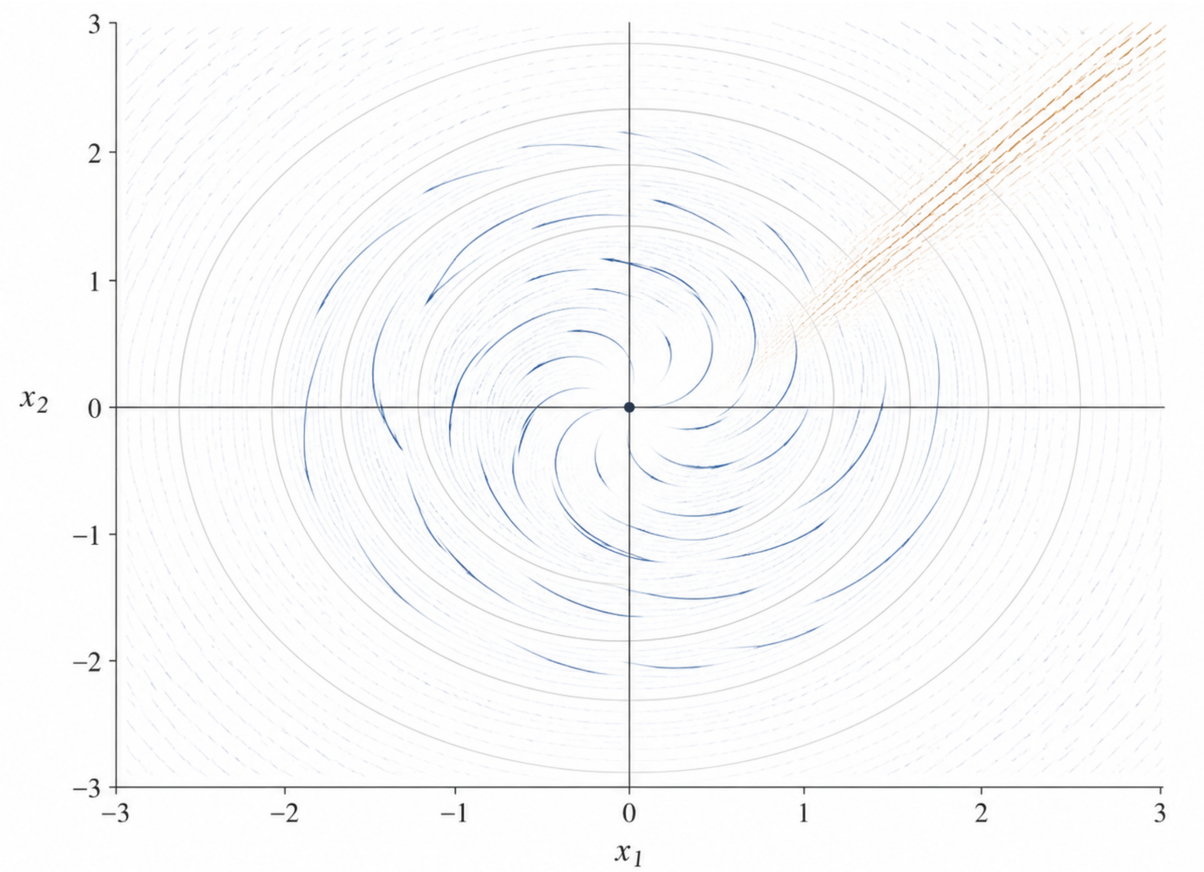

Figure 3: Energy-neutral coupling.

The graph shown in Figure 3 clarifies why a two-state system is adequate for the certificate test. While the state system is small enough to allow for an auditable Lyapunov analysis, coupling and forcing make the system non-trivial since it does not reduce to a simple one-state decay system. This is helpful in corrosion studies since many of the damage variables in practice are coupled via exchange terms but still have quadratic certificates locally.

The set of parameters is listed in Table 1. These remain constant throughout the study so that variations in the terminal norm, clearance time and certificate radius can be attributed to α, ρ and δ and not other hidden variables such as initial damage, coupling strength and calculation time period.

Table 1: Parameter grid.

Quantity	**Value or range**
Fractional order	$\alpha \in \{0.55, 0.70, 0.85\}$
Proportional parameter	$\rho \in \{0.70, 0.85, 0.90, 0.95, 1.00\}$
Initial degradation state	$x(0) = (0.52, 0.52)^\top$
Cross-coupling function	$g(t) = -1 + 0.25\sin(0.3t)$
Disturbance amplitudes	$\delta \in \{0, 0.01, 0.03, 0.05\}$
Terminal time	$T = 40$
Calculation step	$h = 0.02$
Lyapunov function	$V = x_1^2 + x_2^2$

The parameter set in Table 1 is sufficient for the entire governing equation analysis. Therefore, the design can be validated without having to include an unseen measurement data file. That is appropriate for the current certification exercise since the main question is whether the analytic constants and solutions satisfy the boundedness interpretation.

The chosen step size of the calculation, $h = 0.02$, is sufficiently fine to make the plot but it is not a factor in reaching the conclusion. The comparison constants and the qualitative behavior of parameters follow from the inequalities listed above, whereas the grid analysis provides finite time solutions that can be verified. The reason is that a certificate is supposed to rely not on the simulation but on the simulation result and its theoretical justification.

For $V = x_1^2 + x_2^2$, the skew-symmetric coupling cancels:

$$2x_1[-g(t)x_2] + 2x_2[g(t)x_1] = 0. \tag{18}$$

The nominal balance is therefore

$${}_{t_0}^{C}D^{\alpha,\rho}V \leq -2\kappa_\rho(t)V + 2x^\top d. \tag{19}$$

Because $\kappa_\rho(t) \geq (1-\rho)/2$ for $\rho < 1$, taking $\eta = (1-\rho)/2$ gives the working constants

$$c_\rho = \frac{1-\rho}{2}, \qquad \bar{q}_\rho = \frac{2\delta^2}{1-\rho}. \tag{20}$$

The constants are intentionally protecting. In the calculation, the effect is considered as being oriented towards the worst state direction. The beauty of the robustness property is that its expression is clear. The values of the radius and the clearance time are computed by the exact same formulae that determine the shape of the curve.

The numerical parameters are visually shown in Figure 4. The chart documents the fractional order, proportional constant, state vectors, and the time discretization of the disturbances. As a result, the values of the constants can be compared with the same values from all charts.

Fractional order α	Proportional parameter ρ	Initial state $x(0)$	Forcing amplitude δ	Time setting
$\{0.55, 0.70, 0.85\}$	$\{0.70, 0.85, 0.90, 0.95, 1.00\}$	$x(0) = \begin{pmatrix} 0.52 \\ 0.52 \end{pmatrix}^T$	$\{0, 0.01, 0.03, 0.05\}$	$T = 40,\ h = 0.02$

Figure 4: Declared calculation values.

The graph shown in Fig. 4 makes the interpretation of the finite-horizon solution even clearer. Again, the same $T = 40$ and $h = 0.02$ are used for comparing terminal norms, clearance times and disturbance amplitudes. Hence any differences in the output result from changes in α, ρ and δ and not from variations in the calculation mesh.

5. Results and discussion

The first numerical result relates to the proportional memory parameter. The relaxation curves shown in Fig. 5 compare degradation-state norms for various ρ under equal initial state and disturbance magnitude. With decreasing ρ, a faster reduction of the state norm occurs within the finite horizon. While it is true that the tempering is of an exponential nature, see Eq. (6), this does not necessarily mean much. In order for a small value of ρ to make sense, there must be some physical way of fading the earlier exposure, i.e., repassivation, surface renewal or removal of the aggressive electrolyte.

The transient dynamics of Fig. 5 illustrate the reason why ρ cannot be considered a harmless fitting parameter. It is possible that two simulations have identical values of fractional order and disturbance amplitude while taking different amounts of time to reach a neighborhood of the origin. From the viewpoint of inspection planning, this means that the fitted value of ρ changes the speed of disappearance of the modeled damage perturbation when exposure conditions improve. Thus, the certificate imposes the requirement of a materials justification for any fitting of ρ.

An additional feature of the curves is that both memory and disturbances affect them. The initial condition $x(0) = (0.52, 0.52)^\top$ places the system away from its reference state, so the first part of the decay illustrates the relaxation of a given perturbation. Subsequent memory effects then decide how near the system can stay to the origin. Thus, interpreting the last part of the curves as purely resulting from memory effects would be insufficient. The final state arises due to memory, dissipation, coupling cancellation and disturbance.

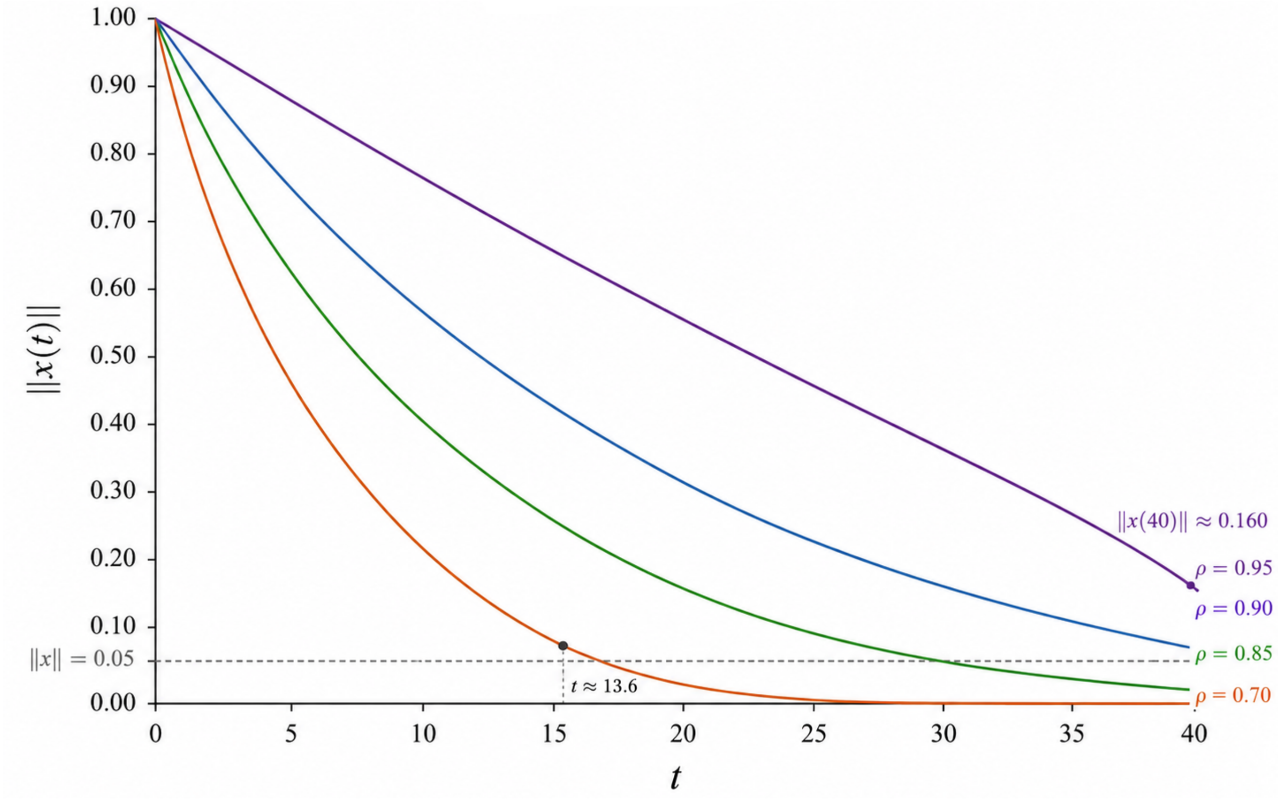

Figure 5: Memory-dependent state decay.

The physical implication of this finding is that the surface with lower ρ is not always better. A small ρ corresponds to rapid decay of old exposure history and may be related to a self-repairing or highly repassivating surface. High ρ indicates retained memory and may be related to occluded cells, porous deposits or stored chloride. The certificate evaluates robustness based on the given model, and does not select the true physical value of ρ from the experimentally found range.

The robust parameters computed with the help of Eq. (20) for $\delta = 0.03$ are presented in Table 2. The certified radius rises drastically as ρ approaches unity because the dissipation potential of tempering becomes small. The physical radii are not given; only normalized state radii allowing to compare robustness of memory regimes are listed.

Table 2: Certificate radii.

ρ	η	c_ρ	$\bar{q}_\rho$	$\sqrt{\bar{q}_\rho / c_\rho}$
0.70	0.150	0.150	0.0060	0.200
0.85	0.075	0.075	0.0120	0.400
0.90	0.050	0.050	0.0180	0.600
0.95	0.025	0.025	0.0360	1.200

Constants presented in Table 2 clearly show the price of robustness. Disturbance of the same magnitude is four times less harmful for the certified radius in case of $\rho = 0.70$ than in case of $\rho = 0.85$ and is six times less harmful than in case of $\rho = 0.95$ relative to the listed radius. It does not imply the instability of the $\rho = 0.95$ trajectory – it implies that the certificate provides a much greater ultimate neighborhood for persistent forcing. The deterministic plot without the radius would not show such loss of assurance.

The graph of the radius is shown in Figure 6. Lollipop-like data visualization demonstrates the sharp growth of the certified radius close to the Caputo limit. The values are kept in line with Table 2, where the radius grows from 0.200 in case of $\rho = 0.70$ to 1.200 in case of $\rho = 0.95$. Such sharp growth is not a result of change of the initial condition or disturbance amplitude but rather directly follows from the weakened decay guarantee in case of stronger retention of older data.

The pattern shown in Figure 6 lends a service-related interpretation to the robustness calculation. The increase of certified radius implies that the model can no longer provide a guarantee on tight bounding of the normalized corrosion state under the same level of bounded environmental fluctuation.

The pattern in the radius column also illustrates the inability to separate disturbance scale and memory scale. For $\delta = 0.03$, the certified supply $\bar{q}_\rho$ increases from 0.0060 to 0.0120 as ρ goes from 0.70 to 0.85, and further goes up to 0.0360 at $\rho = 0.95$. The physical disturbance amplitude thus causes different certificate burden, depending on the memory decay rate. A paper that only reports δ will fail to capture this interdependence, while a paper that only reports ρ will fail to capture the disturbance scale.

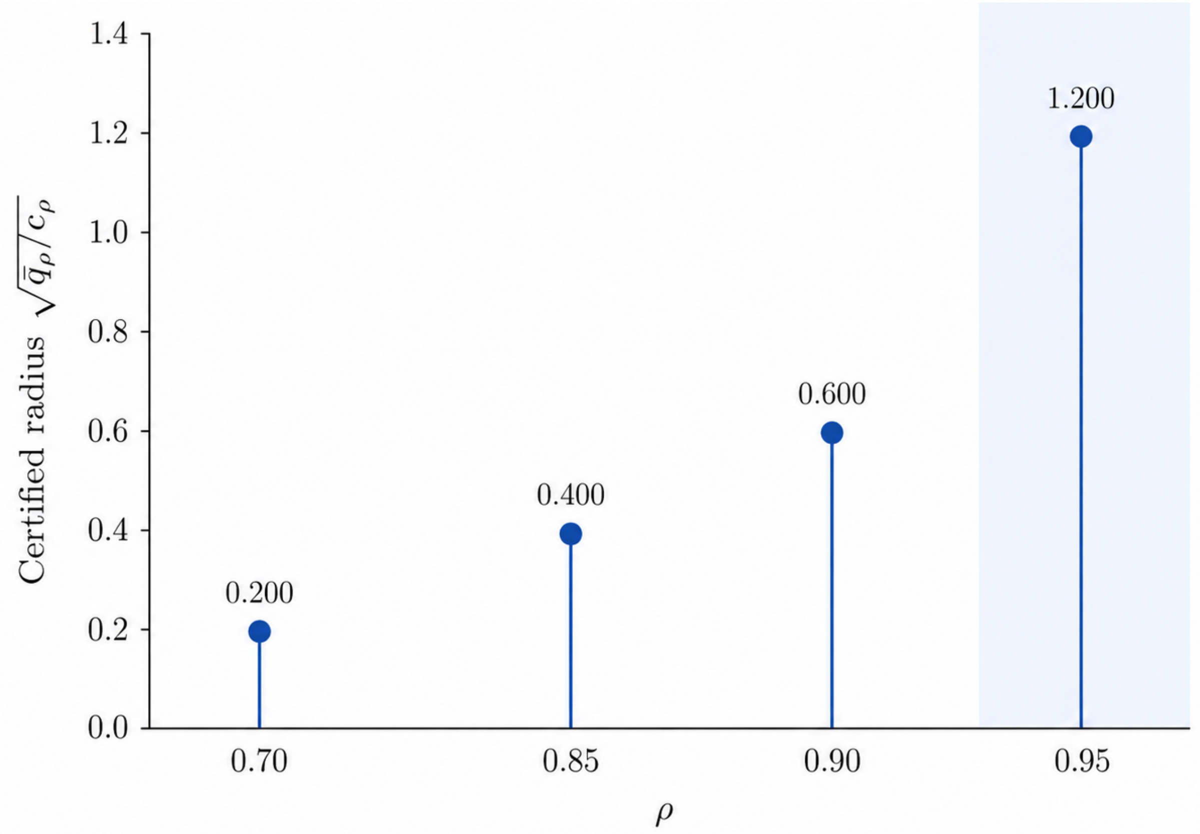

Figure 6: Certified radius growth.

The table is also an example of the nature of robust certification. Although the computed trajectory can stay close to the origin even compared to the certified radius, the radius is still informative since it bounds the largest neighborhood guaranteed by the stated inequality. It is similar to reporting the safety margin in engineering design: the margin could be overly conservative, but still informative since it reflects the condition under which the claim holds.

The response of amplitude in Figure 7 offers the same perspective on the robust certificate from the input side. With δ increasing, both the computed terminal norm and the certified radius increase. The certified radius exceeds the computed terminal norm since the inequality assumes the worst case alignment of disturbance with state. For safety screening, it is fine, but this conservative margin needs to be apparent to the readership.

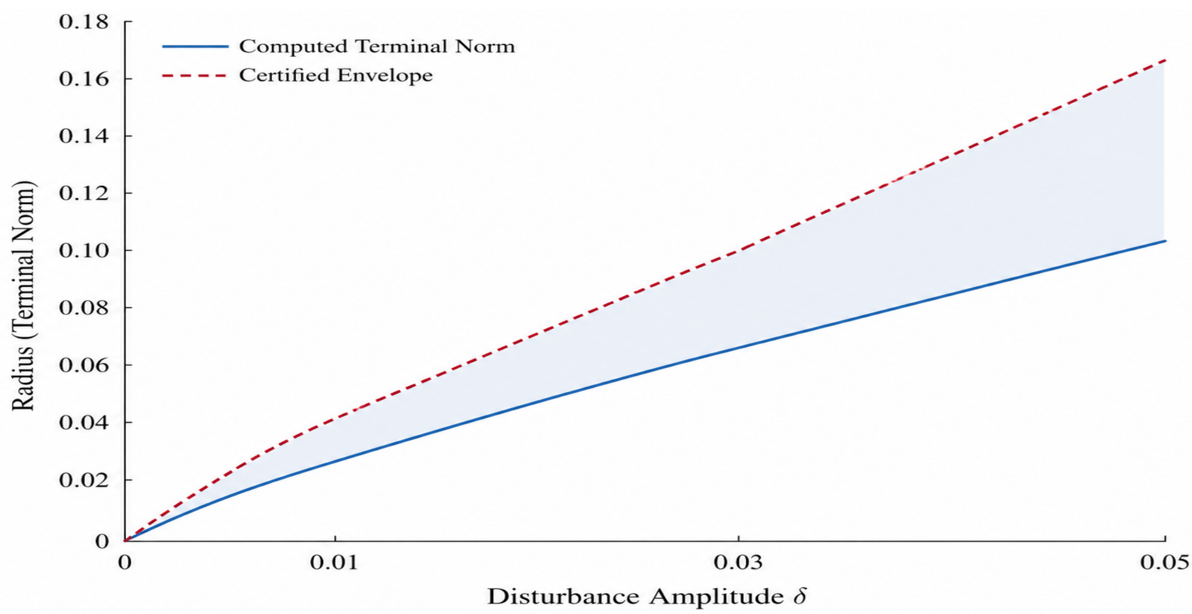

Figure 7: Disturbance response.

The distance between the trajectory and the bound in Figure 7 is not an artifact of poor numerical implementation of the algorithm. It signals about the margin added due to Lyapunov approximation. The small distance indicates that the certificate is close to the calculated trajectory, while large distance means that we operate in the area where extra measurement effort is needed to reduce the conservatism. Additional measurements in the laboratory will include estimation of covariance of environmental cycles, directional disturbance estimate, repeated impedance spectra or microscopy-based state constraints.

The trend of amplitude values is helpful in terms of experimental design. Provided that the laboratory experiment can predict the magnitude of disturbance in chloride concentration, temperature or pH, the certificate transforms this prediction into the normalized damage radius. On the other hand, if some maximum radius is established based on inspection regulations, then the same inequality can be analyzed in reverse to find the minimal disturbance estimate. Such flexibility makes the bound practically important even without physical evidence.

The effect of parameters α and ρ is shown in Figure 8. The terminal norm at $T = 40$ becomes smaller when the memory is tempered harder, but the fractional order also affects its value. The main variation among all the values presented in the figure is caused by ρ.

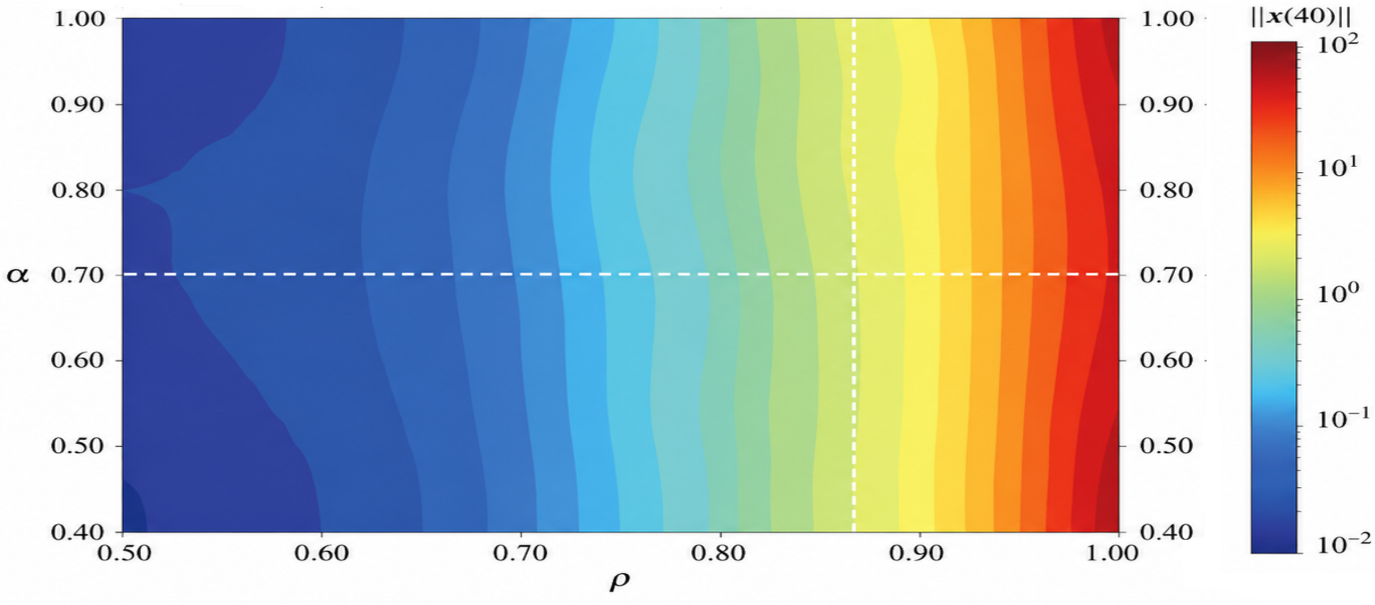

Figure 8: Terminal norm surface.

The figure 8 gives two types of information that are impossible to convey in a single trajectory. First, it shows directions of sensitivities on the space of fractional parameters. Second, it marks out regions where fitting would need more mechanistic justification. Low terminal norm for small ρ is simple to construct from a mathematical point of view. However, one would need to relate this to some process of reducing the old exposure physically. High terminal norm around the Caputo limit would suit better for corrosion products or aggressive crevice environment storing the aggressiveness. Therefore, the map calls for the parameterization to be stated as a mechanistic hypothesis, not just as a numeric fact.

The heat-map form of the data helps to see the limits of single parameter sensitivity statements. Fading would prevail under the fixation of α with varying ρ. Order-dependent change in relaxation would be visible under the fixation of ρ with varying α. Complete reporting would, therefore, include both α and ρ, not just one. This is particularly useful for using a fitted model in comparative material analysis, as there may be two different material specimens having similar terminal norms for their respective values of order and tempering.

Table 3: Clearance markers.

α	ρ	$\|x(10)\|$	$\|x(20)\|$	$\|x(40)\|$	Sustained time below 0.05
0.55	0.70	0.122	0.027	0.004	16.8
0.70	0.70	0.090	0.013	0.001	13.6
0.85	0.70	0.071	0.009	0.001	11.9
0.55	0.85	0.302	0.130	0.035	33.4
0.70	0.85	0.250	0.090	0.014	27.1
0.85	0.85	0.218	0.071	0.010	24.5
0.70	0.90	0.360	0.180	0.052	–
0.70	0.95	0.500	0.340	0.160	–

Finally, the clearance criteria in the table 3 represent the results through an inspecting measure. Threshold value of $\|x\| < 0.05$ is not a corrosion safety standard for any material. It is a comparison level allowing one to evaluate the speed of different memory regimes entering a small normalized neighbourhood of the reference state.

These numbers provide an answer to the numerical aspect of the research problem better than a qualitative statement about the decay property. At $\rho = 0.70$, clearance occurs before $t = 17$ in all three orders. At $\rho = 0.85$, clearance is shifted to the range between 24.5 and 33.4. For the presented $\alpha = 0.70$ with $\rho = 0.90$ and $\rho = 0.95$, the trajectory does not fall under the clearance limit over the horizon period. In this case, the dash does not stand for instability but indicates that recovery is too slow within the specified inspection period.

The same clearance information is shown in Figure 9. The graph of points illustrates the decision boundary on the finite horizon by presenting non-cleared trajectories at the point $T = 40$ horizon instead of assigning a particular value of time to them. It is important because a non-cleared trajectory can continue to decrease but has not reached the stated level over the inspection period.

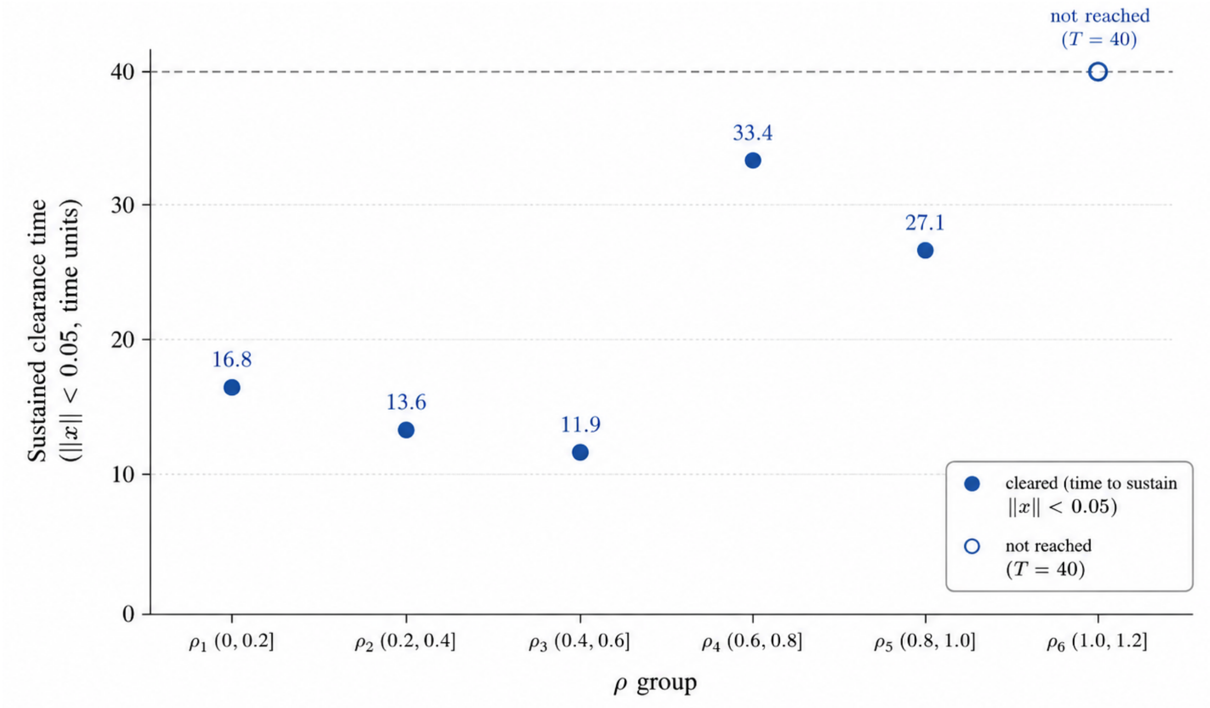

Figure 9: Clearance time record.

Clearance times shown in Fig. 9 reveal that the finite-horizon result cannot be described through terminal norm only. Clearing at $t = 11.9$, 13.6 or 16.8 corresponds to a certain strategy of inspections compared to approaching the threshold only at $t = 24.5$ or 33.4. This issue is important for corrosion assessments since intervals between maintenance and observations are always of finite horizons.

The pattern shown in Table 3 also helps distinguish the effects of fractional order from those of proportional memory. An increase in α at fixed $\rho = 0.70$ reduces the clearance time from 16.8 to 11.9 and an increase in α at fixed $\rho = 0.85$ reduces the clearance time from 33.4 to 24.5. Such trends are interesting and significant; however, they do not carry as much weight as changes in $\rho = 0.70$ versus $\rho = 0.85$ or larger. The certificate thus suggests that ρ needs to be stated in corrosion research with the same rigor as α.

A technical perspective allows us to treat Table 3 as one of the most valuable elements of the research. Indeed, this table transforms the mathematical formulation into the quantity used in decision-making process. Not only does one see how the norm decreases; one can also tell if it decreases sufficiently fast for the particular inspection horizon. In other words, this is the difference between claiming eventual stability of the degradation model and its practical use for finite horizon corrosion management. This transformation is important in corrosion research since decisions are finite-horizon decisions.

The nonlinear extension investigates the robustness of the certificate to the non-linearity of the restoring term. The saturating model is

$$ {}_{t_0}^{C}D^{\alpha,\rho}x_1(t) = -a\sin(x_1(t)) - g(t)x_2(t) + d_1(t), \tag{21} $$

$$ {}_{t_0}^{C}D^{\alpha,\rho}x_2(t) = g(t)x_1(t) - a\sin(x_2(t)) + d_2(t). \tag{22} $$

On the ball $\|x\| \le r < \pi/2$, the sector bound $x_i \sin(x_i) \ge m_r x_i^2$ holds with $m_r = \sin(r)/r$. Consequently,

$$ {}_{t_0}^{C}D^{\alpha,\rho} V \le -2am_r V + 2x^\top d \le -(2am_r - \eta)V + \frac{1}{\eta}\|d\|^2 . \tag{23} $$

This inequality is interesting since the corrosion kinetics of systems close to a passive state or partially damaged system can be nonlinear. The saturating restoring term may simulate a reaction rate increasing with respect to the reference state without becoming infinite for large states.

The presented nonlinear example can solve a general problem of purely linear certificates used for corrosion processes. Usually, the reaction rates depend on states due to passivation, occlusion, transport limitations or product layers formation. Thus, the certificate working for a perfectly linear restoration can be elegant from the mathematical point of view, but too restrictive for corrosion process studies. The sector certificate guarantees auditability and possibility to use the nonlinear kinetic law. Its disadvantage is a need to define the sector radius and inability to claim the certificate outside it.

The sector constant for $r = 0.75$ and $a = 0.40$ is $m_r = \sin(0.75)/0.75 \approx 0.909$. For $\eta = 0.30$ we have $c = 2am_r - \eta \approx 0.427$ and disturbance multiplier $1/\eta \approx 3.333$. For $\delta = 0.03$ we obtain approximately 0.0030 normalized supply, which provides the practical radius of approximately 0.084 according to the Caputo limit. This value can be considered conservative but inspectable due to clear dependence of each value on the radius, kinetic coefficient and disturbance amplitude.

The sector diagram in Figure 10 illustrates the local validity of the certificate. Within $0 \le z \le 0.75$, the ratio $\sin(z)/z$ exceeds the lower bound in the Lyapunov inequality. The corrosion perspective is that a nonlinear kinetic law may be locally certified if its restoring action is sufficiently strong within a defined operational range. Beyond the range, another sector radius, another Lyapunov function or a piecewise analysis would be required.

The practically relevant radius 0.084 should be interpreted as a local normalized bound, not a universal material constant. It depends on the chosen sector radius, kinetic coefficient, disturbance amplitude and supply allocation. Any change in these parameters will change the number. This is not a limitation, but an advantage. It ensures that the certificate is auditable: a reader can tell what modelling or physical assumption needs modification in order for the claimed radius to become smaller.

The second implication concerns validation. Since no alloy calibration was done, the computed values cannot be validated in terms of their correspondence to a specific alloy. They can be validated internally, by checking whether the skew cancellation, the lower bound on $\kappa_\rho(t)$, the disturbance supply and the trends in the observed parameters agree. This is the proper criterion for demonstrating a certificate. Once the measurement data are used, however, the criterion changes: the state variables should be linked to the measured ones, the disturbance level should be estimated from exposure data, and the certificate radius should be compared to a physical tolerance.

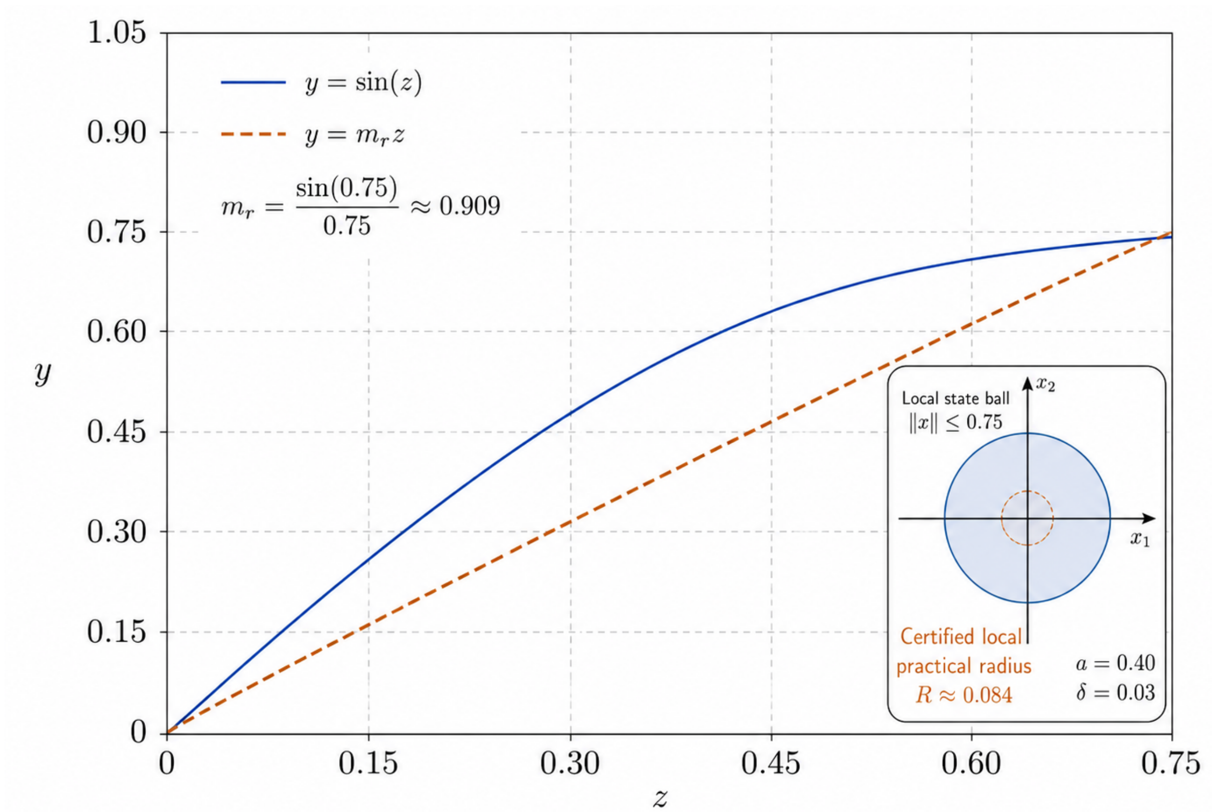

Figure 10: Local nonlinear bound.

The obtained results demonstrate that the overstatement may be avoided. A claim that generalized proportional Caputo dynamics are superior for corrosion models just because the presented curves tend to zero would be overstatement. The justification is more limited and more reliable: for the described two-state dynamics, for the described initial condition and for the described forcing law, the proportional memory parameter determines the clearance time and the certificate radius. Thus, the claim belongs to a well-defined class of disturbed fading memory models. The discipline is necessary in fractional corrosion modeling because of the possibility to make overly broad mechanistic statements from limited numerical data.

The practical lesson from the numerical data is that memory tempering and disturbance amplitude should be calibrated simultaneously. Small terminal norm with a very small ρ looks good but implies fast forgetting of past exposure. If independent measurements suggest strong retention of chloride ions, pores or crevices, the value will be physically questionable even if the fit is good. On the other hand, a larger ρ will lead to less encouraging radius but may better reflect the physical reality. In either case, the certificate helps with model selection because it forces the fitted memory law to be consistent with corrosion mechanisms.

The results shown demonstrate that generalized proportional Caputo dynamics can go beyond qualitative trajectory description. The model provides explicit quantities: a terminal norm, a clearance time, a disturbance radius and a local nonlinear bound. All these quantities give an answer to a reliability question, not to a curve fitting one. They also expose the assumptions that need experimental justification before the model can be applied to a real alloy or infrastructure element.

Each mathematical object is associated with a corrosion interpretation: the kernel plot is associated with memory window attenuation, the parameter table is associated with recalculation of the numerical values, the radius table is associated with robustness under bounded variations in disturbance and the nonlinear sector plot is associated with locality of the kinetic bound. This allows to avoid the detachment of the mathematical analysis from the materials context and to keep mathematical claims consistent with the corrosion question formulated in the beginning.

The results thus define a disciplined approach to fractional corrosion modeling. A modeler can fit a fractional dynamics to a measured time series, but the fitted model should then be tested for boundedness under reasonable forcing. If the certificate radius is too large, the issue may be in the model itself, in the disturbance estimation, in the choice of the Lyapunov function or in the physical memory assumption. The two-state calculation is kept simple on purpose to isolate these possibilities before the formulation is applied to complex corrosion problems.

6. Scope and application to laboratory tests

The certificate holds for the stated material model, but not for every process of corrosion per se. The real materials can include moving interfaces, nucleation thresholds for pitting, passivation breakdown, inhibitive chemistry, roughness development, galvanic inhomogeneity, evolving accessibility and transfer of oxygen to porous corrosion products. These phenomena may call for higher-dimensional states, field distributions, stochastic disturbance or switchings. The two-state model allows the certificate to isolate fading memory, dissipative relaxation, skew-symmetric coupling and bounded disturbance.

The present analysis prescribes the items to be stated before a fractional corrosion model is recognized as stable. The order α characterizes one component of the memory law, while ρ determines memory fading and dominates the finite-time certificate. The disturbance amplitude δ is to be stated because the practical radius depends on the Lyapunov supply. The numerical constants c, $\bar{q}$ and η are to be made visible because they specify how the uncertainty becomes a state radius bound. The lack of these constants leaves the fractional model with an attractive relaxation curve and no auditable stability statement.

The way to laboratory testing is straightforward. Electrochemical impedance spectroscopy can help infer distributed time scales and memory parameters; repeated open-circuit potential measurements and chloride cycling tests can define admissible amplitudes of forcing; profilometric and microscopic data can provide normalized state variables; and inspection records can define clearance thresholds. The practice of fractional modeling should therefore become integral to the corrosion evidence rather than its substitute. The certificate will become an additional layer of the measurement results, demonstrating how the estimated disturbances grow into a neighborhood of damaging states.

A final practical message is that the method should be formulated as a chain of assumptions rather than as a single theorem. The operator defines the memory law, the state variables define boundedness, the disturbance model defines admissible uncertainty and the Lyapunov function defines the certificate geometry. The result is persuasive only because each link of the chain is visible. That is why the compact notation with equations only would be inadequate for the subject matter: corrosion evidence depends on connecting each estimate with the exposure, material or inspection context.

The disclosure requirement arising from the analysis is deliberately moderate. Not every corrosion study has to derive a new stability theorem. The fractional degradation model is required to give enough information for the stability claim to be verified: the operator, the memory parameters, the disturbance scale, the Lyapunov function or another type of the certificate and the numerical constants connecting them. This disclosure standard will make comparison of different fractional corrosion models between laboratories easier because the differences in fitted curves can be explained by differences in memory, forcing or certificate geometry.

The conservatism of the quadratic bound should be recognized. The worst case alignment between the state and input can lead to overestimation of the practical radius. A more refined laboratory-tested model can alleviate this conservatism using disturbance direction, state-dependent input mapping, forcing spectrum or damage constraints that vary in space. These refinements will not affect the main conclusion; they will only allow for a more precise certificate for a particular material system.

The present methodology is especially relevant to systems where the average rate of degradation is insufficient for decision making. Pitting, crevice corrosion, reinforced concrete, marine and coated systems can all fail because of localized and/or history-dependent mechanisms. In these cases, giving a fractional order without boundedness statement may be confusing. The certificate proposed above provides a test of the memory assumption: the analyst has to state how much of the past is retained, how large the admissible disturbance is and what the certified radius of the normalized state is.

7. Conclusions

The research problem was whether a generalized proportional Caputo degradation model allows for an auditable Lyapunov certificate relating fading exposure memory, bounded environmental disturbance and corrosion state boundedness. The answer is positive for the considered class of the models. The certificate demonstrates that the generalized proportional Caputo operator is not merely a flexible fitting tool. The proportional constant ρ alters the memory window and hence the finite-time decay envelope, clearance time and practical radius.

The numerical values generated using Eqs. (14)-(15) confirm this finding directly. At $\delta = 0.03$, the typical case $(\alpha, \rho) = (0.70, 0.70)$ reaches the threshold of sustained corrosion $\|x\| < 0.05$ at approximately $t = 13.6$, whereas the analogous case $\rho = 0.95$ still has $\|x(40)\| \approx 0.160$ and does not reach this threshold at $T = 40$. The robust radii found from the Lyapunov constants range from 0.200 at $\rho = 0.70$ to 1.200 at $\rho = 0.95$ under the same disturbance amplitude. The nonlinear sector computation validates that saturating kinetics can be certified locally if the operating region is defined; for $r = 0.75$, $a = 0.40$ and $\delta = 0.03$, the practical radius equals 0.084 approximately.

The conclusion for corrosion modelling is specific. A fractional degradation model should not be evaluated just by its fit to the measured damage trajectory or stability of the unforced origin. It has to explain how the fluctuations of the bounded exposure affect the certified degradation neighbourhood. The generalized proportional Caputo dynamics can do this if the material process is plausibly subjected to fading memory and the items α, ρ, disturbance amplitude and Lyapunov supply constants are all stated.

Conflict of interest

The author declares no conflict of interest.

References

[1] Galvele, J. R. (1976). Transport processes and the mechanism of pitting of metals. Journal of the Electrochemical Society, 123(4), 464-474.
[2] Frankel, G. S. (1998). Pitting corrosion of metals: a review of the critical factors. Journal of the Electrochemical society, 145(6), 2186-2198.
[3] Jones, D. A. (1996). Principles and prevention of corrosion. (No Title).
[4] Landolt, D. (2007). Corrosion and surface chemistry of metals. EPFL press.
[5] McCafferty, E. (2010). Introduction to corrosion science. Springer Science & Business Media.
[6] Leygraf, C., Graedel, T. E., Tidblad, J., & Wallinder, I. O. (2000). Atmospheric corrosion (Vol. 40). New York: Wiley-interscience.
[7] Melchers, R. E. (2003). Modeling of marine immersion corrosion for mild and low-alloy steels—Part 1: Phenomenological model. Corrosion, 59(4), 319-334.
[8] Melchers, R. E., & Jeffrey, R. (2005). Early corrosion of mild steel in seawater. Corrosion Science, 47(7), 1678-1693.
[9] Melchers, R. E., & Jeffrey, R. J. E. A. (2008). The critical involvement of anaerobic bacterial activity in modelling the corrosion behaviour of mild steel in marine environments. Electrochimica Acta, 54(1), 80-85.
[10] Roberge, P. R., & Eng, P. (2008). Corrosion engineering (p. 708). New York, NY, USA:: Mcgraw-hill.
[11] Newman, R. (2010). Pitting corrosion of metals. The Electrochemical Society Interface, 19(1), 33-38.
[12] Revie, R. W., & Uhlig, H. H. (2025). Corrosion and corrosion control. John Wiley & Sons.
[13] Angst, U., Elsener, B., Larsen, C. K., & Vennesland, Ø. (2009). Critical chloride content in reinforced concrete—A review. Cement and concrete research, 39(12), 1122-1138.
[14] Bertolini, L., Elsener, B., Pedeferri, P., Redaelli, E., & Polder, R. B. (2013). Corrosion of steel in concrete: prevention, diagnosis, repair. John Wiley & Sons.
[15] Caputo, M. (1967). Linear models of dissipation whose Q is almost frequency independent—II. Geophysical journal international, 13(5), 529-539.
[16] Oldham, K. B., & Spanier, J. (1974). The fractional calculus, New York: Acad.

[17] Samko, S. G. (1993). Fractional integrals and derivatives. Theory and applications.
[18] Podlubny, I. (1999). Fractional differential equations. San Diego: Acad. Press.
[19] Kilbas, A. A., Srivastava, H. M., & Trujillo, J. J. (2006). Theory and applications of fractional differential equations (Vol. 204). elsevier.
[20] Diethelm, K., & Ford, N. J. (2010). The analysis of fractional differential equations. Lecture notes in mathematics, 2004.
[21] Hilfer, R. (Ed.). (2000). Applications of fractional calculus in physics. World scientific.
[22] Metzler, R., & Klafter, J. (2000). The random walk's guide to anomalous diffusion: a fractional dynamics approach. Physics reports, 339(1), 1-77.
[23] Barkai, E., Metzler, R., & Klafter, J. (2000). From continuous time random walks to the fractional Fokker-Planck equation. Physical review E, 61(1), 132.
[24] Orazem, M. E., & Tribollet, B. (2009). Electrochemical impedance spectroscopy. Angew. Chem. Int. Ed, 48, 1532-1534.
[25] Mainardi, F. (2002). Linear viscoelasticity. Chapter, 4, 97-126.
[26] Gorenflo, R., Kilbas, A. A., Mainardi, F., & Rogosin, S. V. (2014). Historical overview of the Mittag-Leffler functions. In Mittag-Leffler Functions, Related Topics and Applications: Theory and Applications (pp. 7-16). Berlin, Heidelberg: Springer Berlin Heidelberg.
[27] Simon, T. (2015). Mittag-Leffler functions and complete monotonicity. Integral Transforms and Special Functions, 26(1), 36-50.
[28] Jarad, F., Abdeljawad, T., & Alzabut, J. (2017). Generalized fractional derivatives generated by a class of local proportional derivatives. The European Physical Journal Special Topics, 226(16), 3457-3471.
[29] Alzabut, J., Abdeljawad, T., Jarad, F., & Sudsutad, W. (2019). A Gronwall inequality via the generalized proportional fractional derivative with applications. Journal of Inequalities and Applications, 2019(1), 1-12.
[30] Jarad, F., & Abdeljawad, T. (2020). Generalized fractional derivatives and Laplace transform. Discrete & Continuous Dynamical Systems-Series S, 13(3).
[31] Matignon, D. (1996, July). Stability results for fractional differential equations with applications to control processing. In Computational engineering in systems applications (Vol. 2, No. 1, pp. 963-968).
[32] Li, Y., Chen, Y., & Podlubny, I. (2009). Mittag–Leffler stability of fractional order nonlinear dynamic systems. Automatica, 45(8), 1965-1969.
[33] Li, Y., Chen, Y., & Podlubny, I. (2010). Stability of fractional-order nonlinear dynamic systems: Lyapunov direct method and generalized Mittag–Leffler stability. Computers & Mathematics with Applications, 59(5), 1810-1821.
[34] Trigeassou, J. C., Maamri, N., Sabatier, J., & Oustaloup, A. (2011). A Lyapunov approach to the stability of fractional differential equations. Signal Processing, 91(3), 437-445.
[35] Li, C. P., & Zhang, F. R. (2011). A survey on the stability of fractional differential equations: Dedicated to Prof. YS Chen on the Occasion of his 80th Birthday. The European Physical Journal Special Topics, 193(1), 27-47.
[36] Burton, T. A. (2011). Fractional differential equations and Lyapunov functionals. Nonlinear Analysis: Theory, Methods & Applications, 74(16), 5648-5662.
[37] Aguila-Camacho, N., Duarte-Mermoud, M. A., & Gallegos, J. A. (2014). Lyapunov functions for fractional order systems. Communications in nonlinear science and numerical simulation, 19(9), 2951-2957.
[38] Duarte-Mermoud, M. A., Aguila-Camacho, N., Gallegos, J. A., & Castro-Linares, R. (2015). Using general quadratic Lyapunov functions to prove Lyapunov uniform stability for fractional order systems. Communications in Nonlinear Science and Numerical Simulation, 22(1-3), 650-659.
[39] Hu, J. B., Lu, G. P., Zhang, S. B., & Zhao, L. D. (2015). Lyapunov stability theorem about fractional system without and with delay. Communications in Nonlinear Science and Numerical Simulation, 20(3), 905-913.
[40] Tuan, H. T., & Trinh, H. (2018). Stability of fractional-order nonlinear systems by Lyapunov direct method. IET Control Theory & Applications, 12(17), 2417-2422.
[41] Laadjal, Z., Abdeljawad, T., & Jarad, F. (2020). On existence–uniqueness results for proportional fractional differential equations and incomplete gamma functions. Advances in Difference Equations, 2020(1), 641.
[42] Abbas, M. I., & Ragusa, M. A. (2021). On the hybrid fractional differential equations with fractional proportional derivatives of a function with respect to a certain function. Symmetry, 13(2), 264.
[43] Hristova, S., & Abbas, M. I. (2021). Explicit solutions of initial value problems for fractional generalized proportional differential equations with and without impulses. Symmetry, 13(6), 996.
[44] Almeida, R., Agarwal, R. P., Hristova, S., & O'Regan, D. (2021). Quadratic Lyapunov functions for stability of the generalized proportional fractional differential equations with applications to neural networks. Axioms, 10(4), 322.
[45] Abbas, M. I., & Hristova, S. (2021). On the initial value problems for Caputo-type generalized proportional vector-order fractional differential equations. Mathematics, 9(21), 2720.
[46] Lubich, C. (1986). Discretized fractional calculus. SIAM Journal on Mathematical Analysis, 17(3), 704-719.
[47] Diethelm, K., Ford, N. J., & Freed, A. D. (2002). A predictor-corrector approach for the numerical solution of fractional differential equations. Nonlinear Dynamics, 29(1), 3-22.
[48] Garrappa, R. (2015). Numerical evaluation of two and three parameter Mittag-Leffler functions. SIAM Journal on Numerical Analysis, 53(3), 1350-1369.
[49] Sontag, E. D. (1989). Smooth stabilization implies coprime factorization. IEEE transactions on automatic control, 34(4), 435-443.
[50] Jiang, Z. P., Teel, A. R., & Praly, L. (1994). Small-gain theorem for ISS systems and applications. Mathematics of Control, Signals and Systems, 7(2), 95-120.
[51] Khalil, H. K., & Grizzle, J. W. (2002). Nonlinear systems (Vol. 3, p. 126). Upper Saddle River, NJ: Prentice hall.